

CONFORMATIONAL HETEROGENEITY OF APOAZURIN MUTANT M121L FROM *Pseudomonas* *aeruginosa*: A FLUORESCENCE STUDY

ZHANG Hong-jie^{1,2}

(1. Institute of Biophysics, The Chinese Academy of Sciences, Beijing 100101, China; 2. Institut für Physikalische Chemie der Westfälischen
Wilhelms-Universität Münster, Schloßplatz 4/7, 48149 Münster, Germany)

Abstract: Unfolding of *Pseudomonas aeruginosa* apoazurin has been suggested to be more complex than the Zn²⁺ substituted form. This complexity was investigated using a mutant M121L with urea as denaturant. Although the equilibrium unfolding/refolding showed a two-state transition, its kinetic behaviour was complex and could be best understood as two interconvertible conformations coexisting in solution. One conformation (N₁), which was unfolded fast, was found to be refolded independently through a three-state mechanism with a fast-populated intermediate on its pathway, while refolding of the other (N₂), which was unfolded slow, was dominantly through N₁ folding pathway, then to be isomerised into N₂. Adding of the extraneous ligand Zn²⁺ could integrate these two native conformations into a unique complex and the corresponding unfolding kinetics was reduced to a monophasic process. This provides new insight on the unfolding behaviour of this protein.

Key Words: Urea denaturation; Unfolding; Azurin; Fluorescence; Stopped-flow

1 Introduction

Azurin, a type I blue copper protein, functioned as an electron carrier in a variety of denitrifying bacteria^[1]. The oxidized form of this protein displays an intense optical absorption around 600 nm and an unusually small hyperfine splitting in the electron paramagnetic resonance spectrum.

There is only one Trp residue, Trp48, pointing with its side chain to the centre of the hydrophobic core of the protein. It endows the protein with unique fluorescence/phosphorescence properties, which has been utilized in several time-resolved fluorescence/phosphorescence studies^[2,3]. It has been confirmed that the apparent multi-exponential decay of the fluorescence/phosphorescence originates from conformational heterogeneity and not from a contaminating protein. For apoazurin, the conformational difference has been suggested that it arose from the protonization/deprotonization of His 35.

Although the conformational heterogeneity of

apoazurin has been investigated both in crystals and in solutions, its effect on the physicochemical properties has not been thoroughly investigated. In the extensive folding studies performed previously, the static and kinetic stepwise signal changes observed during heat or denaturant-induced unfolding were still arbitrarily ascribed to the existence of an intermediate on its unfolding pathway^[4,5]. A metal ligand, such as Zn²⁺, was considered to stabilize the metal binding sub-domain, so the complex unfolding of apoazurin became a simple first-order transition. Clearly, this interpretation is, however, only justified as long as one assumes a single unique three-dimensional structure of apoazurin in native state.

Received: Jan 13, 2004

Corresponding author: Zhang Hong-jie, Present address is Institute of Biophysics, The Chinese Academy of Sciences, 15 Datun Road, Beijing 100101, China. Tel: +86(10)64837257, Fax: +86(10)64872026, Email: hjzhang@sun5.ibp.ac.cn

The limitations of the former wt apoazurin unfolding studies^[4,5] are apparent due to its irreversible transitions. Within the abundant literature related to protein folding mechanisms, several papers focused on the multiple conformation characters of the two-step unfolding processes for proteins^[6-8]. Among these the Chevron plot analysis plays an important role. The logarithms of the observing rate constants for the unfolding and refolding phases that connect smoothly with each other in the transition zone reflect a reversible folding reaction that limits both unfolding and refolding. If two or more chevrons are observed, vertically displaced from each other, a parallel folding mechanism is possible as remarked by Wallace and Matthews^[8]. This has been exemplified in the parallel folding studies for dihydrofolate reductase and staphylococcal nuclease.

In order to avoid the folding irreversibility of wt azurin, the mutant M121L in apo and Zn²⁺ substituted forms, which showed excellent reversible properties, were employed to carry out the thermodynamic and kinetic experiments and simulation. The results suggested that the apo form of this protein adopt at least two distinguishable and interchangeable conformations and that the biphasic unfolding processes were the result of two conformations' independent unfolding. It was also showed that the ligand Zn²⁺ was able to integrate the two conformations into a single one.

2 Materials and Methods

2.1 Materials

P. aeruginosa azurin mutant M121L protein was a gift from Dr. Brengelmann. Its construction and expression were essentially the same as that described by Germanas et al^[9]. Holo-protein purity was checked by SDS-Page, using 15% polyacrylamide gel. A single band at 14 ku was observed for azurin mutant. The apo protein was prepared using 100 mmol/L thiourea^[5,10]. Its

purity was checked by both UV-visible spectrum at 620 nm and molecular size-exclusion chromatography utilizing a Bio-Rad SEC 125-5 column. Protein concentration was determined by absorption using an extinction coefficient, $\epsilon_{280\text{ nm}} = 8\ 834\ \text{M}^{-1}\text{cm}^{-1}$. Zinc substituted azurin mutant Zn-azurin M121L was prepared by dialysing the apo protein against 1 mmol/L ZnSO₄ solution in 50 mmol/L acetate buffer, pH 5.0, followed with dialysis to bulk buffer at least twice.

2.2 Methods

Fluorescence emission spectra were measured in 1 cm cells using a Spex Fluoromax spectrophotometer. Emission spectra were excited at 280 nm and recorded from 300 to 400 nm with an increment of 1 nm and a response time of 1 s. Excitation and emission slits of 5 nm each were employed during all spectra measurements. The slow unfolding kinetics were also monitored in the Spex Fluoromax spectrophotometer using manual mixing in a 3 ml cuvette and spectral line width of 2.6 nm.

The refolding and fast unfolding kinetics were monitored with a SFM-3 stopped-flow from Bio-Logic. The samples were excited at 280 nm and the emission signals above 305 nm were detected using a wavelength cut-off filter. A dead-time of 10.8 ms resulting from the flow rate conditions was calculated by the instrument itself.

Evaluation of the isothermal unfolding curve was performed numerically according to Santoro and Bolen's procedure^[11] using the equations:

$$Y = \frac{Y_N + m_N[\text{urea}] + (Y_D + m_D[\text{urea}]) \cdot Q}{1 + Q} \quad (1)$$

$$Q = \exp\left(-\frac{\Delta G_D^0(\text{H}_2\text{O}) - m_G[\text{urea}]}{RT}\right) \quad (2)$$

Y_N and Y_D are the intercepts, and m_N and m_D are the slopes of the pre- and post-unfolding baselines respectively. [urea] is the denaturant concentration. $\Delta G_D^0(\text{H}_2\text{O})$ is the standard Gibbs free energy change for the unfolding in absence of urea, and m_G is the slope of the plot of ΔG_{app}^0 versus urea concentration, according to:

$$\Delta G_{\text{app}}^0 = \Delta G_{\text{D}}^0(\text{H}_2\text{O}) - m_{\text{G}}[\text{urea}] \quad (3)$$

The digitized kinetic traces for the fast and slow unfolding processes were analyzed with Equation (4) respectively:

$$F_t = (F_0 - F_{\infty}) \exp(-kt) + F_{\infty} \quad (4)$$

where F_t and F_{∞} are respectively the signal at time t , and the signals of the final states for the fast or slow processes. F_0 is the initial signal at time of zero. k is the unfolding kinetic constant for the fast or slow processes respectively. For the refolding process, the data were also fitted to a single exponential equation, Equation (4).

The activation free energy for the unfolding reaction, $\Delta G_{\text{u}}^{0\neq}$, was calculated using Equation (7). It is based on the transition state theory according to Eyring^[12].

$$\ln k_{\text{u}}^{\text{H}_2\text{O}} = \ln \frac{\kappa k_{\text{b}} T}{h} - \frac{\Delta G_{\text{u}}^{0\neq}}{RT} \quad (5)$$

where $k_{\text{u}}^{\text{H}_2\text{O}}$ is the unfolding rate constant at 0 mol/L urea, k_{b} is the Boltzmann constant, T is the absolute temperature in Kelvin, h is the Planck constant, R is the gas constant, and κ is the transmission factor which is arbitrarily set to unity.

2.3 Kinetic simulation

The three-state folding kinetic scheme with a fast-populated intermediate on its pathway was tested for compatibility with the experimental data. $\text{U} \rightleftharpoons \text{I} \rightleftharpoons \text{N}$

where U, I and N represent the fully unfolded, partially folded intermediate and native states respectively. The unfolding rate constant k_{u} increases with the final urea concentration increase according to:

$$\ln k_{\text{u}} = \ln k_{\text{u}}^{\text{H}_2\text{O}} + (m_{\text{N-TS}}/RT)[\text{urea}] \quad (6)$$

where R is the gas constant, T is the temperature, $k_{\text{u}}^{\text{H}_2\text{O}}$ is the unfolding rate constant in buffer and $m_{\text{N-TS}}$ is the slope of the logarithm of rate constants versus urea concentrations in $\text{kJ} \cdot \text{mol}^{-1} \cdot \text{M}^{-1}$. The latter is proportional to the difference in buried

surface area between the native (N) and transition state^[13-16]. The refolding rate could be expressed by the product of the populated fraction of I (f_{I}) and the refolding rate constant of the intermediate (k_{IN}) to the native state. As f_{I} can be expressed in terms of the equilibrium constant between U and I (K_{UI}), the refolding rate can be written as Equation (7) or (8):

$$k_{\text{f}} = f_{\text{I}} k_{\text{IN}} = \frac{K_{\text{UI}}}{1 + K_{\text{UI}}} \cdot k_{\text{IN}} \quad (7)$$

$$\ln k_{\text{f}} = \ln \frac{K_{\text{UI}}^{\text{H}_2\text{O}} e^{(-m_{\text{U-I}}/RT)[\text{urea}]}}{1 + K_{\text{UI}}^{\text{H}_2\text{O}} e^{(-m_{\text{U-I}}/RT)[\text{urea}]}} + \ln \left(K_{\text{IN}}^{\text{H}_2\text{O}} e^{(-m_{\text{I-N}}/RT)[\text{urea}]} \right) \quad (8)$$

The measured folding/unfolding rate constant (k_{obs}) reflects contributions from both the folding and unfolding as

$$k_{\text{obs}} = k_{\text{f}} + k_{\text{u}} \quad (9)$$

The curved chevron plot at low denaturant concentrations can be fitted to Equation (9) combined with Equations (6) and (8).

3 Results

3.1 Equilibrium denaturation transitions of apo and zinc substituted forms of azurin mutant M121L in urea

The fluorescence probe, Trp-48, was utilized to detect equilibrium unfolding/refolding of apo mutant in urea at 20°C (Figure 1). The curves are superimposable with a single sigmoidal transition, indicating that under the conditions the folding of this mutant is fully reversible. Numerical analysis using a two-state model gives apparent thermodynamic parameters of $\Delta G_{\text{D}}^0(\text{H}_2\text{O}) = 26.2 \text{ kJ} \cdot \text{mol}^{-1}$, $C_{\text{m}} = 3.71 \text{ mol/L}$, $m_{\text{G}} = 7.06 \text{ kJ} \cdot \text{mol}^{-1} \cdot \text{M}^{-1}$. Here the term "apparent" refers to the fact that the equilibrium unfolding of the apoprotein could just apparently be described as a two-state model. The real process is more complex, as demonstrated in the kinetic study of this paper.

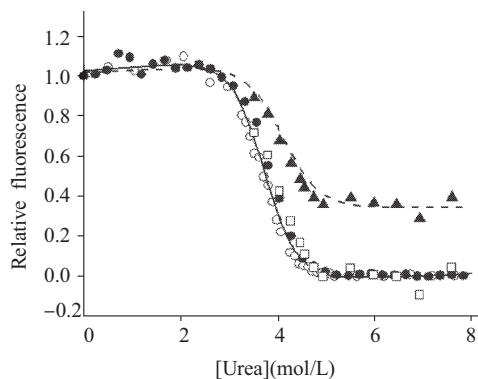


Fig.1 Apoazurin mutant M121L unfolding transition curves and simulations. The open and filled circles refer to the relative fluorescence intensity changes at 308 nm for steady unfolding and refolding respectively, after 24 h incubation at 20°C. The excitation was set at 280 nm. Protein concentration was 6.4 mg/L in 20 mmol/L sodium acetate buffer, pH 5.1. The solid line refers to the fitted curve according to Equation (1). The filled triangles refer to the relative signal changes of the fast phase during the unfolding kinetic processes, where the total signal change of the fast and the slow phases at high urea concentrations are normalized to unity. The emission intensity above 305 nm was collected using a stopped-flow apparatus. The protein concentration used was 0.03 g/L. The open squares are the transformed data from the fast unfolding signals, where the coefficient 1/0.34 was applied to each data point after baseline correction. The dash line indicates the calculated quasi-steady state unfolding transition curve for the fast unfolding based on the three-state model. The corresponding parameters are taken from Table 1 after the pre- and post-unfolding baseline corrections

For comparison, the Zn^{2+} substituted mutant was also studied. A single sigmoidal transition occurs between 4 and 6.5 mol/L urea (Figure 2). Curve fitting analysis gave its thermodynamic parameters of $\Delta G_D^0(H_2O)=33.8 \text{ kJ}\cdot\text{mol}^{-1}$, $C_m=5.17 \text{ mol/L}$ and $m_G=6.53 \text{ kJ}\cdot\text{mol}^{-1}\cdot\text{M}^{-1}$. Clearly, binding of ligand resulted in an increase in protein stability.

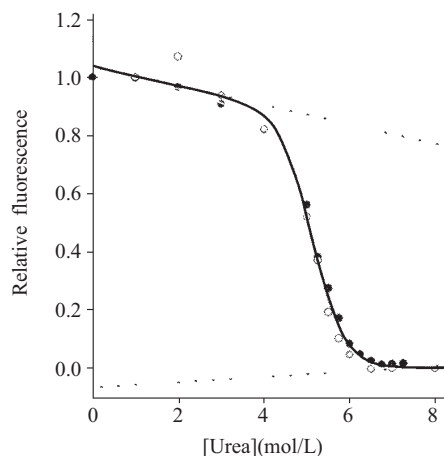


Fig.2 Zinc-substituted azurin mutant M121L unfolding transition curve. The filled and open circles refer to the relative fluorescence intensities at 308 nm for unfolding and refolding, respectively, after 24 h incubation at 20°C. Excitation was set at 280 nm. Protein concentration was 5.4 mg/L in 20 mmol/L sodium acetate buffer, pH 5.1. The solid line refers to the fitted curve according to Equation (1). The dotted lines correspond to the pre- and post-unfolding baselines

3.2 Unfolding kinetics of apo azurin mutant M121L

Similar to wt apoazurin^[4], the unfolding kinetics of the mutant M121L also showed a biphasic process, a fast phase with 66% fluorescence signal decrease finished within manual mixing dead-time (about 15 s) and a slow process with the other 34% signal decrease, where the whole of fast and slow signal changes are normalized to unity. The fast phase can be followed using a stopped-flow apparatus. The time course of the signal changes can be fitted to a single phase at 6.175 mol/L urea using the rate constant of 7.1 s^{-1} (insert plot of Figure 3 line E). The relative signal changes of this fast process at different urea concentrations were also measured and are shown in Figure 1 (filled triangles). It is clear that the kinetic relative amplitude changes are constant in the post-transition urea concentration region, and are less than that from equilibrium unfolding measurement under the same

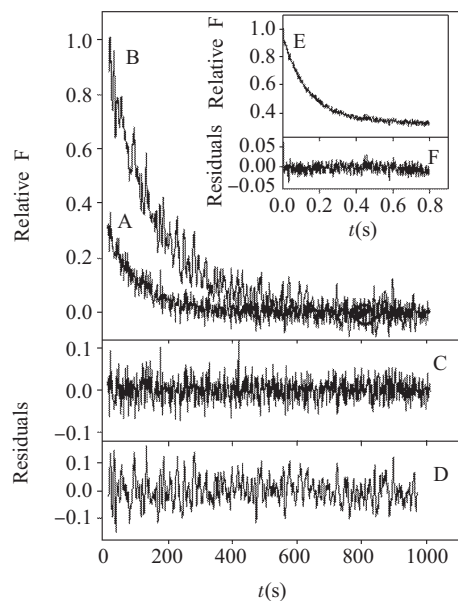


Fig.3 Apo and zinc-substituted azurin mutant M121L unfolding kinetics. Line A represents unfolding process for the apo protein at a concentration of 6.4 mg/L in 6.25 mol/L urea by manual mixing; Line B represents unfolding for the zinc-substituted protein with concentration of 5.4 mg/L in 6.94 mol/L urea by manual mixing. The signals were collected with 1 data point/s. In both cases the protein signals at zero concentration of denaturant were scaled to unity while the final signals were scaled to zero. Line C and Line D show the fitting qualities of line A and B to a first order kinetic Equation (4) respectively. The solution conditions were 20 mmol/L sodium acetate buffer solution with pH 5.1 at 20°C. Inserting plot shows fast unfolding kinetics of apo azurin mutant M121L monitored by stopped-flow apparatus. Line E represents the unfolding kinetics in 6.175 mol/L urea solution. Line F shows the fitting quality to a monophasic process. Fluorescence was excited at 280 nm and signals above 305 nm were collected with 1 data point/ms using the filter-cutting primes. The protein concentration used was 0.03 g/L. Other conditions were the same as in the manual mixing experiments

urea concentration within the transition zone. This suggests that the equilibrium unfolding position is reached through a complex mechanism. The kinetics of the other 34% signal change within post-transition region can be followed by manual mixing as shown in Figure 3 line A, and the data can also be fitted to a single exponential process

with an unfolding rate constant of 0.0103 s^{-1} at 6.25 mol/L urea solution. Using the refolded sample, the same unfolding kinetic processes with the same signal fractions for the fast and slow phases were given (data not shown). No obvious change of the relative amplitudes of the fast and slow unfolding occurs within this urea concentration range (Figure 4). The linear relationships of the logarithm of the fast and slow unfolding rate constants versus urea concentrations at post-transition region are clear (Figure 5). The unfolding rate constant of the slow process in buffer is calculated as $k_{N_2-U}^{\text{H}_2\text{O}} = 2.13 \times 10^{-7} \text{ s}^{-1}$, the slope, $m_{N_2-TS_2} = 4.22 \text{ kJ} \cdot \text{mol}^{-1}$ according to Equation (6), and the unfolding activation free energy, $\Delta G_{N_2-U}^{0\ddagger} = 109 \text{ kJ} \cdot \text{mol}^{-1}$ according to Eyring Equation (5) (see Table 1). These kinetic parameters for the fast unfolding process will be given below by combining with the corresponding refolding data (see Table 1).

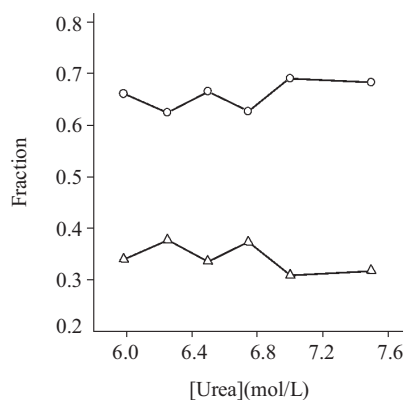


Fig.4 Relative amplitudes of the fast and the slow unfolding processes of the apoazurin mutant M121L versus urea concentrations at the post-transition region. Circles refer to the relative amplitudes of fast unfolding process, and triangles refer to the slow unfolding process. The relative amplitudes of the slow process (f_s) were obtained from manual mixing experiments, and the relative amplitudes of the fast process (f_f) were calculated by $1 - f_s$, where the total signal changes of the fast and slow processes were as unity

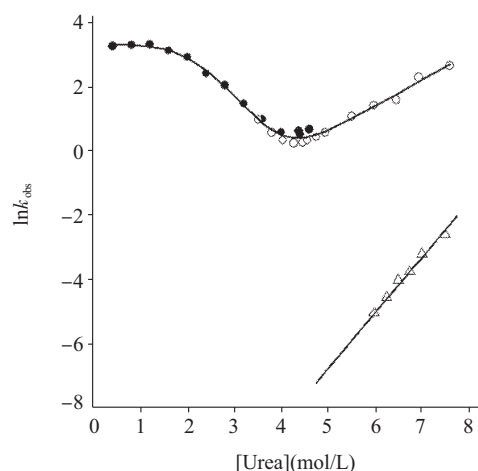


Fig.5 Effects of urea concentration on unfolding and refolding rate constants of apoazurin mutant M121L. The filled circles refer to the fast refolding. The open circles and triangles indicate the fast and slow unfolding, respectively. Other conditions were the same as in Figure 3. The fast unfolding and refolding processes were simulated with an intermediate model (solid line). The corresponding parameters were taken from Table 1

Table 1 Kinetic parameters for the folding of apoazurin M121L

$\Delta G_{U-N_i}^0(\text{H}_2\text{O})^a(\text{kJ}\cdot\text{mol}^{-1})$	26.9
$K_{U-I}^{\text{H}_2\text{O}}$	70.8 ± 14.4
$k_{I-N_i}^{\text{H}_2\text{O}}(\text{s}^{-1})$	26.3 ± 4.6
$k_{N_i-I}^{\text{H}_2\text{O}}(\text{s}^{-1})$	0.030 ± 0.005
$m_{U-I}(\text{kJ}\cdot\text{mol}^{-1}\cdot\text{M}^{-1})$	4.90 ± 0.37
$m_{I-TS_i}(\text{kJ}\cdot\text{mol}^{-1}\cdot\text{M}^{-1})$	-0.26 ± 0.19
$m_{N_i-TS_i}(\text{kJ}\cdot\text{mol}^{-1}\cdot\text{M}^{-1})$	1.99 ± 0.13
β_i^b	0.74
$\beta_{TS_i}^b$	0.70
$\Delta G_{N_i-I}^{0\#}(\text{kJ}\cdot\text{mol}^{-1})$	80.1
$k_{N_i-U}^{\text{H}_2\text{O}}(\text{s}^{-1})$	$2.13(\pm 0.9)\times 10^{-7}$
$m_{N_i-TS_i}(\text{kJ}\cdot\text{mol}^{-1}\cdot\text{M}^{-1})$	4.22 ± 0.17
$\Delta G_{N_i-U}^{0\#c}(\text{kJ}\cdot\text{mol}^{-1})$	109

^a This value was calculated from Equation (10) using the fitted data at zero concentration of urea. ^b The β values were calculated from the m values listed in the Table, such that $\beta_i = m_{U-I} / (m_{U-I} + m_{I-TS_i} + m_{N_i-TS_i})$ and $\beta_{TS_i} = (m_{U-I} + m_{I-TS_i}) / (m_{U-I} + m_{I-TS_i} + m_{N_i-TS_i})$, respectively, and represent the fraction of native surface area buried in I_1 and TS_1 respectively. ^c Data was calculated from Equation (5). Therefore, no error estimations were given for these data

3.3 Refolding kinetics of apoazurin mutant M121L

Refolding kinetics of apo-protein M121L was performed at the same conditions as for unfolding. The sample was prepared by unfolding the protein in 8 mol/L urea for 1 h, then the refolding was triggered by high fold dilution and the fluorescence signal was monitored. This process could be fitted with a single exponential equation, as shown in Figure 6. In 0.4 mol/L urea

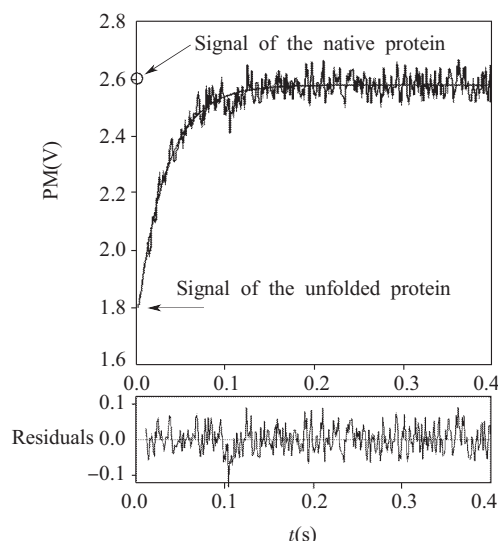


Fig.6 Apoazurin mutant M121L refolding kinetic trace from 8 to 0.4 mol/L urea as monitored by stopped-flow fluorescence intensity increases. The line represents the fit of the data to a monophasic process with rate constant of $(25.8\pm 0.9) \text{ s}^{-1}$. The residuals for the fit are also shown in the lower panel. Other conditions were the same as in Figure 1

conditions, the rate constant is 25.8 s^{-1} with the whole signal recovery. The denaturant concentration effects on the rate constants are shown in Figure 5. The fast unfolding and the refolding rate constants merge together within the transition region, indicating that they are one pair of kinetic processes for the same reaction from different directions. It is labelled as the folding channel. The logarithm of rate constants (k) versus denaturant concentrations in the unfolding limb are linear, while the refolding limb shows curvature, suggesting that this channel involve a complex

molecular mechanism. The three-state model with a fast-populated kinetic intermediate, which is silent to fluorescence change, could be served as an optional model for understanding its kinetic behaviour^[13-16]. Its folding mechanism could be depicted as $U \rightleftharpoons I_1 \rightleftharpoons N_1$, For the slow unfolding limb, no corresponding refolding limb could be observed. where U, I_1 and N_1 stand for unfolded, intermediate and the native state on the folding pathway respectively.

3.4 Unfolding kinetics of Zn substituted azurin mutant M121L

As the unfolding mechanism of apoazurin M121L is complex, the role of metal ligand in this protein is interesting. In order to avoid the complex reduction-oxidisation effect caused by copper ion, the non-functional ligand Zn^{2+} was employed^[4]. The result is shown in Figure 3 at a urea concentration of 6.94 mol/L, the same conditions were used as for the apoprotein. It is clear that the complicated unfolding of apoazurin is reduced to a first order transition. The rate constant is 0.0065 s^{-1} , which is 5 folds slower than the slow phase of unfolding for the apo form under the same conditions, which has a rate constant of 0.033 s^{-1} , (see simulation study). A similar result has been reported for wt Zn-azurin^[4].

3.5 Size-exclusion chromatography of the apoazurin mutant M121L

In order to understand the complex folding mechanism of apoazurin mutant M121L, the possibility of multiple species caused by protein dimerization or oligomerization should be considered. Thus a size-exclusion chromatography experiment was performed as shown in Figure 7. Only one peak was observed, which verified that the complex mechanism is not caused by the dimerization/oligomerization of the apo protein.

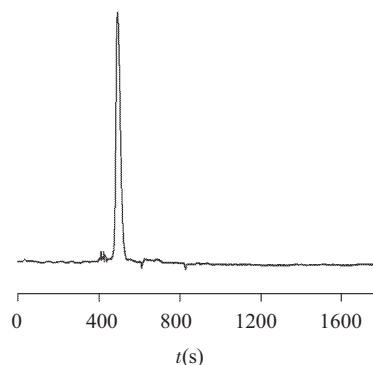


Fig.7 Molecular size-exclusion chromatography of the apoazurin mutant M121L. The elution was performed using a Bio-Rad SEC-125 column and the elution peak was monitored by UV absorbance at 280 nm. The buffer solution was 50 mmol/L Tris-HCl, 1 mmol/L EDTA at pH 5.1

3.6 Simulation of the folding channel of apo protein with three-state model

The kinetic data for the folding channel could be modelled according to the three-state mechanism^[13-16]. It was assumed that the rate of interconversion between unfolded U and intermediate I_1 was fast compared with the stopped-flow dead-time, so that only the pre-equilibrium constant (K_{U-I_1}) can be determined experimentally. The set of six independent variables (K_{U-I_1} , m_{U-I_1} , m_{I_1-TS} , m_{N_1-TS} , $k_{I_1-N_1}^{H_2O}$, $k_{N_1-I_1}^{H_2O}$) that produced the best agreement between observable rates and the values obtained by non-linear least squares fitting are shown in Table 1. The results show that in aqueous solution, the apoazurin mutant M121L folds rapidly to an intermediate that is remarkably stable ($\Delta G_{U-I_1}^0(H_2O)=10.4\text{ kJ}\cdot\text{mol}^{-1}$) and has ~70% of the surface area of the native state buried (calculated from the ratio $\beta_{I_1} = m_{U-I_1} / (m_{U-I_1} + m_{I_1-TS} + m_{N_1-TS}) = 0.74$). The protein then

collapses further into a transition state in which almost the same degree of native surface is buried (calculated from $\beta_{TS_1} = (m_{U-I_1} + m_{I_1-TS_1}) / (m_{U-I_1} + m_{I_1-TS_1} + m_{N_1-TS_1}) = 0.70$). This is consistent with an entropy-limited folding process, where the intermediate I_1 as well as the transition state between I_1 and N_1 are part of the same ensemble of rapidly interconverting compact conformations, and implies that the properties of the transition state between I_1 and N_1 are similar to those of I_1 . The standard Gibbs free energy change for the native N_1 to its intermediate I_1 is calculated as $19.2 \text{ kJ}\cdot\text{mol}^{-1}$, and to the fully unfolded U was as $\Delta G_{U-N_1}^0 = 26.6 \text{ kJ}\cdot\text{mol}^{-1}$. The unfolding activation free energy, $\Delta G_{N_1-U}^{0\#}$, for the fast unfolding channel was calculated as $80.1 \text{ kJ}\cdot\text{mol}^{-1}$.

On the basis of the equilibrium unfolding transition curve reconstruction, it is possible to build the quasi-steady state unfolding transition curve for the fast unfolding channel. Using the simulated thermodynamic parameters and the same baseline for the pre- and post-transition region as drawn from the equilibrium unfolding study, the unfolding transition curve for the fast folding channel can be calculated. Here an assumption of the same baselines for the equilibrium and the quasi-equilibrium transition for the fast folding channel was adopted. This assumption seems reasonable because of the independent unfolding of two interconvertible conformations as showed in Discussion. The calculated transition curve was scaled from 1 at 0 mol/L urea to 0.34 at 8 mol/L urea (dashed line in Figure 1), which fits the measured relative unfolding signal change region. The rebuilt curve fits the fast unfolding transition curve measured by stopped-flow very well (filled triangles in Figure 1).

4 Discussion

4.1 Single sequential unfolding mechanism with unique native conformation is incorrect

The complex unfolding of wt apoazurin has

been observed previously^[4,5]. Its irreversibility hindered deep insight on its folding mechanism. A sequential unfolding mechanism was given arbitrarily. According to it, the fast unfolding product (I) should be an on-pathway partially folded intermediate, which loses 66% fluorescence signal. Further 34% fluorescence decay in the slow phase corresponds to the further unfolding of I to fully unfolded state U.

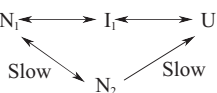
As the folding of this mutant is fully reversible, the refolding must have experienced the same pathway from the reverse direction, i.e., the refolding must first form an partially folded intermediate (I) with 34% fluorescence signal recovery, then refolding further to its native state (N). The observed monophasic refolding could be rational only when the refolding of U to I is the rate-limiting step, i.e. the slow unfolding and refolding rate constants vs. urea concentrations should form a V-like chevron plot. This theoretical expectation is obviously inconsistency with the experimental observation. This inconsistency suggests that the single sequential unfolding mechanism proposed by Engeseth and McMillin, $U \longleftrightarrow I \longleftrightarrow N$ is incorrect.

4.2 Unfolding mechanism of apoazurin mutant M121L

As $U \longleftrightarrow I \longleftrightarrow N$ can't explain the experimental result well, the other option is that it originates from the heterogeneity of the apo protein with at least two species coexistence at the native conditions. One species (N_1) corresponds to the fast unfolding process and the other (N_2) to the slow. Only four possibilities could contribute to it: (1) Two proteins encoded by two different amino acid sequences or caused by side chain modification, i.e. inconvertible; (2) Dimerization/oligomerization of the native state; (3) Metal contamination; (4) Two conformations with slow interconversion.

First let us rule out the Possibility (1). If the two species are inconvertible, the unfolded states should also be heterogeneous. The unfolded state of N_1 is assigned as U_1 and the unfolded state of

N_2 as U_2 . Under this assumption, the equilibrium unfolding transition curve should be contributed from the unfolding of both species N_1 and N_2 independently, and thus should have a two-step transition character with the first transition from N_1 and with the second from N_2 , which is inconsistent with experimental observation of a single sigmoidal transition curve. Moreover, because of the observed monophasic refolding kinetics with the full signal recovery, the refolding rate constants for the U_1 and U_2 should share the same value. As discussed above, from Figure 5, the refolding rate constants of U_2 can't, in any way, merge with the slow unfolding rate constants together, suggesting that the assumed refolding process of U_2 and the slow unfolding process should not be due to the reverse directions of the same N_2 unfolding reaction. This also indicates that the assumption of two coexistent inconvertible species is incorrect. Second, the single elution peak of the apoazurin mutant M121L in size-exclusion chromatography provides direct evidence that the heterogeneity of this protein is not due to the dimerization/oligomerization. Third, the spectral ratio A_{625}/A_{280} of 0.58 for the holo-azurin has been widely used as a purity criterion^[17]. The previous indicated that biphasic unfolding of wt apoazurin was not due to metal contamination, as wt apoazurin could be completely reconstituted by the addition of copper^[4]. For the apoazurin mutant in this study, the monophasic unfolding of Zn^{2+} reconstituted protein also precludes the metal contamination, as the unfolding rate constant of the Zn^{2+} -azurin mutant is 5 folds slower than the slow phase of the apoprotein at the same urea concentration. Only two conformations with slow interconversion are reasonable. Thus the unfolding mechanism can be described as



where N_1 and N_2 are native states of apoazurin M121L with slow interconversion, U is the fully unfolded state, I_1 is the fluorescence silence

intermediate on the N_1 folding pathway. This mechanism suggests that during refolding, only N_1 is folded directly, then to be partially isomerised slowly to conformation N_2 , while during unfolding, N_1 and N_2 experience the parallel pathways.

Besides the on-pathway partially folded intermediate mechanism, the off-pathway intermediate^[16] or transition-moving mechanism^[18] could also be applied to the folding channel simulation. The thermodynamic parameters are essentially the same within experiment error range (data not shown). Thus, the complex unfolding processes of apoazurin mutant M121L is due to multiple conformations of the native structure in solution. Metal ions play an important role in the folding behaviour. Further investigation will focus on defining the type of structural element that results in the phenomenon of coexistence of multiple conformations.

5 Acknowledgements

The author gratefully acknowledges the support in the form of the guest research position funded by the Alexander von Humboldt-Stiftung in the laboratory of Prof. Dr. Hans-Juergen Hinz in Germany. The author also thanks R. Brengelmann for providing protein.

References:

- [1] Nar H, Messerschmidt A, Huber R, van de Kamp M, Canters GW. Crystal structure of *Pseudomonas aeruginosa* apo-azurin at 1.85 Å resolution. *FEBS Lett*, 1992,306(2-3):119-124
- [2] Hansen JE, Steel DG, Gafni A. Detection of a pH-dependent conformational change in azurin by time-resolved phosphorescence. *Biophysical J*, 1996,71(4):2138-2143
- [3] Kroes SJ, Canters GW, Gilardi G, van Hoek A, Visser G. Time-resolved fluorescence study of azurin variants: conformational heterogeneity and tryptophan mobility. *Biophysical J*, 1998,75(5):2441-2450
- [4] Leckner J, Bonander N, Wittung-Stafshede P, Malmström BG, Karlsson BG. The effect of the metal ion on the folding energetics of azurin: a comparison of the native, zinc and apoprotein. *Biochim Biophys Acta*, 1997,1342(1):19-27

